

# Quasi Z-Source Inverter for Pv Power Generation Systems



R.Sathishkumar, R.Velmurugan, Balakrishnan Pappan, J.Booma

**Abstract:** For the enormously increased power demand in the modern world, the existing fossil fuel sources seem to be inadequate to meet the demands. Hence, it is necessary to switch over to use Renewable Energy Sources (RES). Besides the demand concerns, the power generation from fossil fuels causes environmental pollution prominently. As a result, the utilization of RES has been encouraged. When RES is interconnected with the grid, this system becomes an excellent solution to fulfill the power demand of the present scenario. The energy generated from renewable energy sources varies according to seasonal variations. The power generated from RES can be delivered to the load by interconnecting it with the grid. When a small size RES system is connected with the distribution network, it can deliver energy to the isolated zones where the energy cannot be drawn from the conventional network. In this work, the Artificial Neural Network based Maximum Power Point Tracking scheme has been introduced with Photovoltaic (PV) power generation. Also, a bi-directional charger is introduced to overcome the battery issues. The model is evaluated in the MATLAB/SIMULINK package. The performance of the system is analyzed by applying different voltage levels to qZSI. The voltage gain, effectiveness of the scheme, MPPT and the regulation of the voltages are observed.

**Keywords:** qZSI, MPPT, converter, inverter, PV.

## I. INTRODUCTION

The major non-conventional energy sources are PV, wind energy, and hydrogen powered fuel is scientifically acknowledged with the distributed generation. In general, the output of renewable is not regulated and it must be controlled by power converters. The power system reliability makes sure by the working of the converters. Regarding the converter circuit, the old cascaded topology of DC-DC converter and inverter makes the power circuit and controller circuit more complex. Furthermore, price and space needs are also high. The quantity of power electronic converters causes less effectiveness. The solar power generation is suitable and high capable after the arrival of thin-film PV technology, less price,

outstanding efficiency, less weight, elasticity, and easy installation is achieved. In order to interconnect a PV based power source with the grid, we need to add a DC-DC switches which increases the cost of the system. Using those converter configurations would result in a larger stage of power conversion configuration. In order to reduce the configuration, a boosting inverter would be a suitable one. The power conversion and inversion should be done in a single stage to increase the voltage gain of the PV cell. In that case, a Z source inverter would be a suitable one, due to its boosting ability and its inversion ability on a single stage.

## II. QZSI FOR PV SYSTEMS

### A. PHOTOVOLTAIC SYSTEM

A PV array comprises cells that are joined as a series with shunt combinations. Series link of photovoltaic cells will help in raising the voltage of the unit while the shunt connections help in enhancing the current in the solar array. The PV cell output mainly depends on the variation in solar irradiation with temperature. The PV irradiation depends on the environmental condition of the location where it is being placed. Where there is an increase in solar irradiation, it also amplifies the open-circuit voltage. The temperature has an inverse relation to the production of power from the PV. As the temperature tends to increase, the open-circuit voltage will decrease. This is because a rise in temperature exchange the bandgap of the substance and high power is needed. Thus, the effectiveness of the solar cell is lowered. MPPT scheme is applied for enhancing the peak power in the photovoltaic module. Many MPPT methods used to get the maximum output from RES sources. In this work comes under the perturb and observe method.

### B. ANALYSIS OF QUAZI Z SOURCE INVERTER (QZSI)

The conventional z source inverter and quasi z source inverter are illustrated in Fig. 1 and 2. The shoot-through state is not allowed in the conventional as the short circuit will affect the system. The quasi Z source inverter and Z Source inverter is designed with the distinctive inductor, capacitor and diode are joined with the voltage source. This setup will guard the system against short circuit and other power quality problems. The qZSI increases the dc-link voltage and it pulls a steady-state dc from the supply.

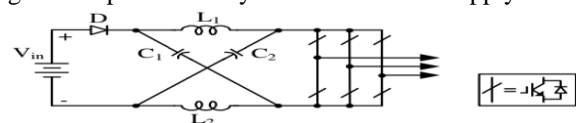


Fig. 1. Z-source inverter topology

Revised Manuscript Received on December 30, 2019.

\* Correspondence Author

**Dr.R.Sathishkumar\***, Associate Professor, Department of Electrical and Electronics Engineering, Pragati Engineering College, Andhra Pradesh, India.

**Dr.R.Velmurugan**, Professor, Department of EEE, Malla Reddy Engineering College For Women, Secunderabad, Hyderabad, India.

**Dr.Balakrishnan Pappan**, Associate Professor, Faculty of Electrical and Electronics Engineering, Malla Reddy Engineering College for Women, Secunderabad, Telangana State. Hyderabad, India.

**Dr.J.Booma**, Assistant Professor, Department of Electronics and Communication Engineering, PSNA College of Engineering and Technology, Dindigul, India.

© The Authors. Published by Blue Eyes Intelligence Engineering and Sciences Publication (BEIESP). This is an open access article under the CC-BY-NC-ND license <http://creativecommons.org/licenses/by-nc-nd/4.0/>

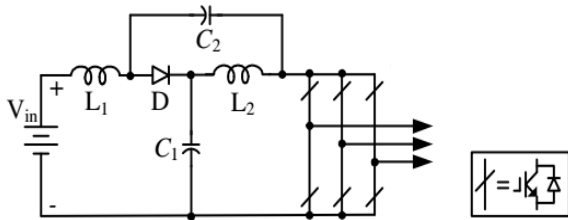


Fig.2. qZSI topology

For the duration T, the period of the shoot-through is  $T_0$ ; the period of the non-shoot-through is  $T_1$ . Here  $T = T_0 + T_1$ ,  $D = T_0 / T$ . From Fig. 3a, this is a representation of the inverter during the period of non-shoot-through states,  $T_1$ .

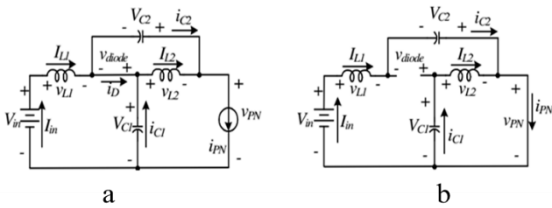


Fig. 3 (a) Non-shoot-through state and (b) shoot-through state

$$\begin{aligned} V_{L1} &= V_{in} - V_{C1}, V_{L2} = -V_{C2} \text{ and} \\ V_{PN} &= V_{C1} - V_{L2} = V_{C1} + V_{C2} \quad V_{diode} = 0. \end{aligned} \quad (1)$$

These derivations are obtained in the paper presented by Li et al (2009).

$$\begin{aligned} V_{L1} &= V_{C2} + V_{in}, V_{L2} = V_{C1}, \text{ and} \\ V_{PN} &= 0 \quad V_{diode} = V_{C1} + V_{C2} \end{aligned} \quad (2)$$

**C. BOOST CONTROL OF A QUAZI Z SOURCE INVERTER**

All the boost control techniques discover for the Z Source Inverter, (i.e. simple boost, maximum boost, and maximum constant boost) it can be made use of qZSI control in the vice versa. The voltage gain of the qZSI is calculated by the formula  $G = \hat{v} \ln / 0.5 \hat{v}_{PN} = MB$ . In order to increase gain, we should reduce the B value and increase the modulation index.

Fig. 4 shows a Variation between modulation index and voltage gain.

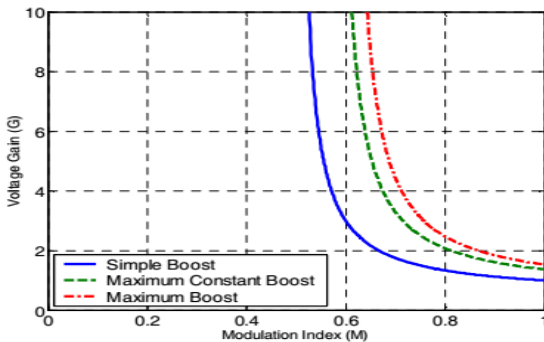


Fig. 4. The variation between the modulation index and voltage gain

The simple boost control possesses uniformly multiply

shoot-through states. The maximum constant boost control gives good results compared to other methods. In this Fig. 5, CRG represents the Current Reference Generator which is used to produce the signals to apply in the PWM circuit with reference to the grid current.

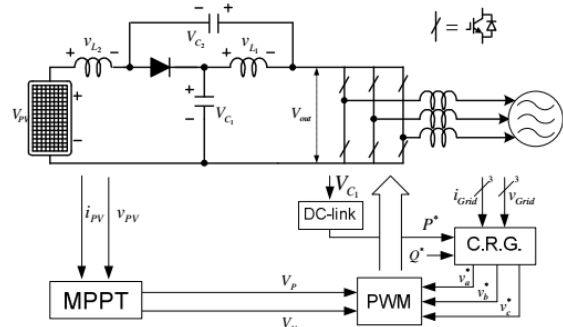


Fig. 5. Block diagram of the photovoltaic system using qZSI

The p-q theory transforms three-phase quantity into two-phase quantity with synchronizing  $\alpha$ -  $\beta$ -0 [These derivations are obtained from Agaki et al (1983).

$$\begin{bmatrix} V_\alpha \\ V_\beta \\ V_0 \end{bmatrix} = \sqrt{\frac{2}{3}} \begin{bmatrix} 1 & -\frac{1}{2} & -\frac{1}{2} \\ 0 & \frac{\sqrt{3}}{2} & \frac{\sqrt{3}}{2} \\ \frac{1}{\sqrt{2}} & \frac{1}{\sqrt{2}} & \frac{1}{\sqrt{2}} \end{bmatrix} \begin{bmatrix} V_a \\ V_b \\ V_c \end{bmatrix} \quad (3)$$

Park transformation is used to get  $\alpha$ - $\beta$  coordinates are transformed to the d-q coordinates

$$\begin{bmatrix} V_d \\ V_q \end{bmatrix} = R(-\omega t) \begin{bmatrix} V_\alpha \\ V_\beta \end{bmatrix}, R(\omega t) = \begin{bmatrix} \cos\omega t & -\sin\omega t \\ \sin\omega t & \cos\omega t \end{bmatrix} \quad (4)$$

If the inverter is linked to the grid from side to side L-filter is depicted in Fig. 5,

$$\frac{d}{dt} R(\omega t) \begin{bmatrix} i_d \\ i_q \end{bmatrix} = \frac{1}{L} R(\omega t) \left[ \begin{bmatrix} V_d \\ V_q \end{bmatrix} - \begin{bmatrix} e_d \\ e_q \end{bmatrix} \right] \quad (5)$$

The above equation changed as below:

$$\frac{d}{dt} \begin{bmatrix} i_d \\ i_q \end{bmatrix} = \frac{1}{L} \begin{bmatrix} V_d \\ V_q \end{bmatrix} + \omega \begin{bmatrix} i_q \\ -i_d \end{bmatrix} - \frac{1}{L} \begin{bmatrix} e_d \\ e_q \end{bmatrix} \quad (6)$$

If the  $V_p <$  carrier frequency, all the control in the three legs are turned on. If  $V_n >$  carrier frequency, all the controls are turned on.

According to the traditional inverter control, the current reference of the proposed work is varied. The synchronization is obtained by determining from the Q axis to reference  $Q^*$ . Whenever it is null, the output is considered to be in phase by Phase-Locked Loop. The D axis and the Q axis frames are combined to regulate the injected power related to the MPPT which operates between the VP and the VN states. The voltage control mode is based on these references. The current reference has been considered based on the D axis deviations. K is the coefficient of D axis variations and it is maintained to zero by varying the duty ratio of the qZSI, which the MPP scheme takes over.

**III. BIDIRECTIONAL BATTERY CHARGER**

A parallel connected battery storage system with an adaptive charge equalizer across the capacitor has been proposed to enhance the voltage balancing of the batteries. To attain the necessary voltage and power in a grid-connected scheme, cascading of battery action is required. Charge imbalance reduces the life cycle of the battery cells, accessible energy, and system performance.

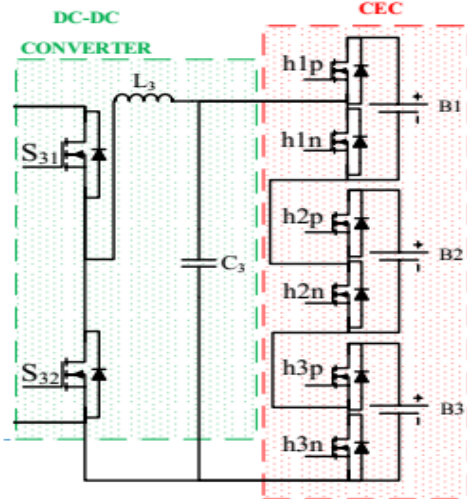


**Fig. 6. Bidirectional control system for battery storage control**

Fig.6. shows the converter with incorporated charge equalization control topology. The scheme is having three low side switches and three high side switches, which are connected with three storage systems.

**A. Battery Charging Mode**

In this mode, the dc-link voltage is maintained using DC-DC switches. A constant dc voltage would be observed in the output of the converters. Hence, the current control would be done by the auxiliary converter. During qZSI to battery mode, the S32 switch is at all times act like a buck converter. To improve the lifetime of the battery, the Constant Current - Constant Voltage (CC-CV) method is selected. The top of the converter will off if the battery is full.

**B. Charge Equalization**

The structure of the storage system gives the chance to avoid a damaged system without disturbing the main system. This capability increases the reliability of the entire scheme. If the battery is fault the low switch will be going to on position, but another switch goes to off mode. So, the faulty module can be simply changed at an appropriate moment. The switching delay to the switch h1n can be determined based on the stack voltages of the battery. The Fig. 7 represents the charge equalization scheme.

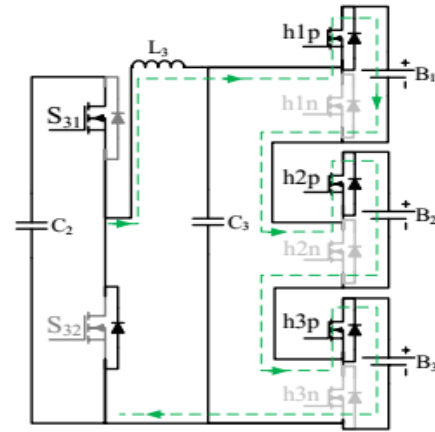


**Fig. 7. Charge equalization scheme**

**C. Charge Equalization Control**

The scheme of the Charge Equalization Control (CEC) is used to change the battery stack by the way of state of charge. The OCV voltage is measured initially before giving charged that is measured by disconnecting load. At the time of battery discharge, the DC-DC switch works as a charge converter. The flow diagram of charge equalization control is illustrated in Fig. 8.

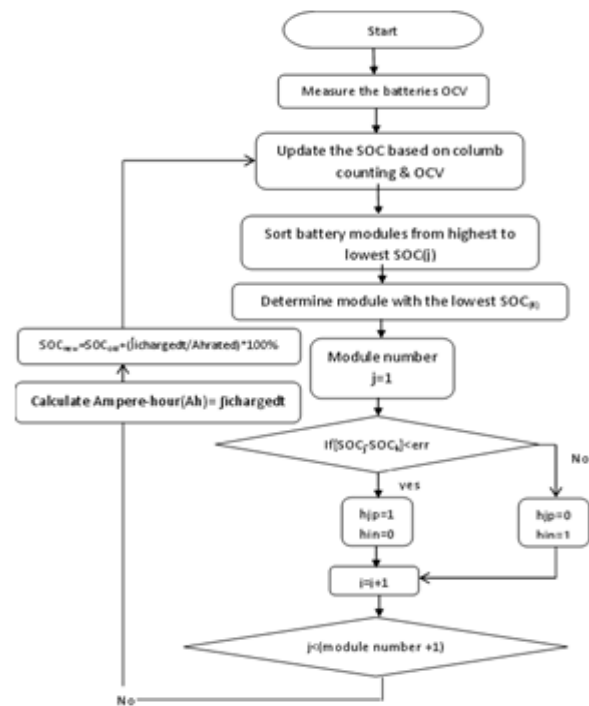


**Fig. 8. Flow chart of the charge equalization control scheme**

**D. Control of the DC-DC converter**

The DC-DC switch either operates in CC scheme or in CV mode based on the battery SoC estimated by the charge equalizer and in both the modes, the switch S31 is controlled. In order to enhance the lifetime of batteries, batteries are release charge by constant current.

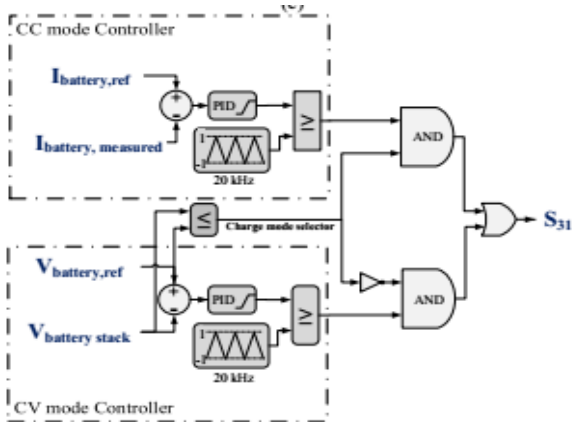


Fig. 9. Control of the DC-DC converter

Fig. 15 depicts the controlling of the DC-DC switch. Here, battery current and measured current values are given input to the PID controller. The AND gate is used, to sum up, the current values with frequency.

IV. IMPLEMENTATION OF QZSI BASED PV SYSTEMS

The block diagram of the planned work is depicted in Fig. 9. In this work, a bidirectional battery charger is connected across the qZSI, which provides equal charge to the battery under critical conditions.

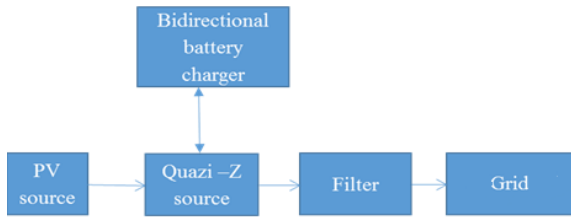


Fig. 10. Block diagram of the proposed scheme

A. Photovoltaic Source details

The Fig. 10 illustrate the I and V graph and the power-voltage graph of the PV array. Fig. 11 presents the current-voltage (IV) graph and the power-voltage graph of a single PV module.

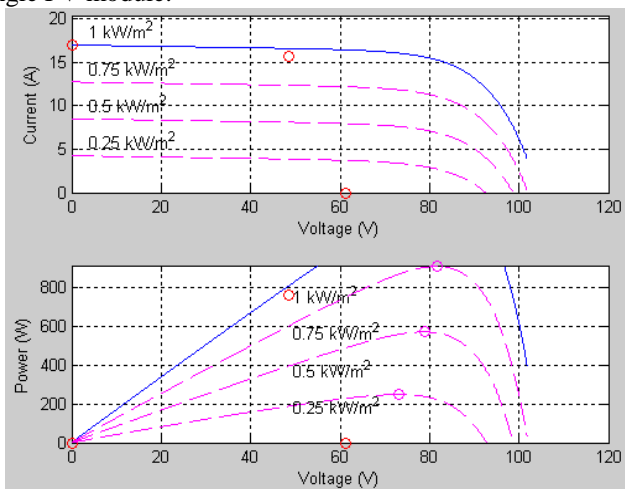


Fig. 11. PV characteristics of an array

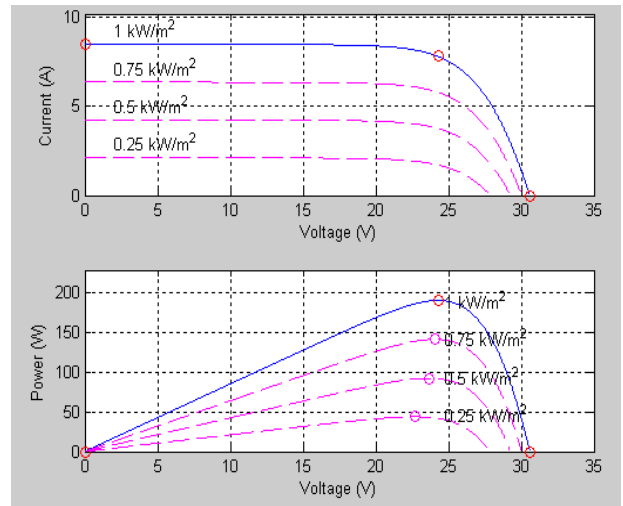


Fig. 12. PV characteristics of a single module

The specifications of the PV panel are provided in Table I. In this work, the Sunpower module is employed. This module contains 96 cells. For each string, there are 5 series-connected modules. Two inductors with the same inductance values of 2.5mH are used and the capacitance value is 1000µF. Fig. 11 shows the PV characteristics of a single module system.

Table I PV specifications

Parameters	Values
Type	Sunpower
Number of cells/unit	96
Number of series unit per string	5
Number of shunt series	2
Voc	64.2V
Isc	5.96A
Vmp	54.7V
Imp	5.58V

B. Circuit Diagram of qZSI

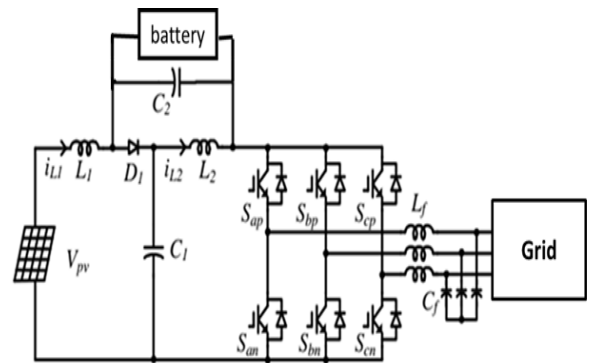


Fig. 13. qZSI based photovoltaic scheme

The proposed work in the PV connected scheme 50 Hz, 230Vrms ac to resistive loads is shown in Fig. 12.

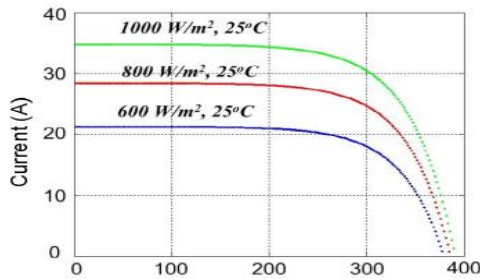


Fig. 14. I-V characteristics

The boosting ability, the PV based on qZSI taken from Li et al (2009). If it works in buck scheme, the smallest amplitude required in qZSI is by

$$\hat{v}_{ln} = \frac{\hat{V}_{PN}}{2} M = \frac{V_{in}}{2} M \quad (7)$$

The largest voltage gain of the qZSI can be determined by

$$G_{max} = \frac{\hat{v}_{ln}}{V_{in}/2} \approx 1.7 \quad (8)$$

The maximum and minimum values of M and B calculated by using below formula

$$M_{min} = \frac{G_{max}}{\sqrt{3}M_{min}-1} \approx 0.875 \quad (9)$$

$$B_{max} = \frac{1}{\sqrt{3}M_{min}-1} \approx 1.94 \quad (10)$$

#### D. SELECTION OF INDUCTOR BANK AND CAPACITOR BANK

In qZSI based photovoltaic scheme,  $f_c$  is 10kHz and the shoot-through frequency  $f_s$  20kHz.  $T_{max}$  can be considered by

$$T_{0\_max} = \frac{2-\sqrt{3}M_{min}}{f_s} \approx 24\mu s \quad (11)$$

The inductance values 1 and 2 are equal here, so it is calculated using the below formula

$$L_1 = L_2 = \frac{V_L \Delta T}{\Delta I} = \frac{mV_{in}}{I_{L\_max} r_c \% 2} T_{0\_max} \approx 356\mu H \quad (12)$$

The two capacitors C1 and C2 are calculated by below formula

$$C_1 = C_2 = 2 \frac{I_C \Delta T}{\Delta(V_{C1} + V_{C2})} = 2 \frac{I_L}{BV_{in} r_v \% 2} T_{0\_max} \approx 310\mu F \quad (13)$$

Table II qZSI component details

Components	Rating
Inductors (L1 & L2)	356μH
Capacitors	310μF

Table II shows the component details of qZSI

#### E. MPPT TRACKING

The PV panel is to be operated to its maximum power and hence, to take out the power generated at its peak, an MPPT based ANN has been proposed. The proposed scheme operates based on the PV parameters like voltage and temperature. The ANN controller is trained with various operating points of the PV panel. The MPPT scheme is shown in Fig. 15. The ANN is trained to operate the qZSI under a constant voltage equivalent to the greatest power generation of the PV panel. The qZSI can be controlled through two individual parameters name by B and shoot through duty control. The ANN alters the duty ratio to operate at the maximum powerpoint.

Due to various operating conditions of the PV panels, the corresponding duty ratio is obtained through training. The ANN controller is trained with a Back-Propagation Learning (BPL) algorithm. The BPL iteration technique is based on gradient descent trying to minimize the network root-mean-square error. The ANN sequence consists of two sets of neural networks in which the first set is trained to predict the solar irradiance. The second stage is trained to predict the optimum output voltage. The first stage output is the output of the second set and it is converted as the duty cycle with a carrier signal. The ANN is targeted to predict the power under various operating conditions with minimized error to target the real-time power and it achieves the maximum power point under all operating conditions for both shaded and non-shaded conditions.

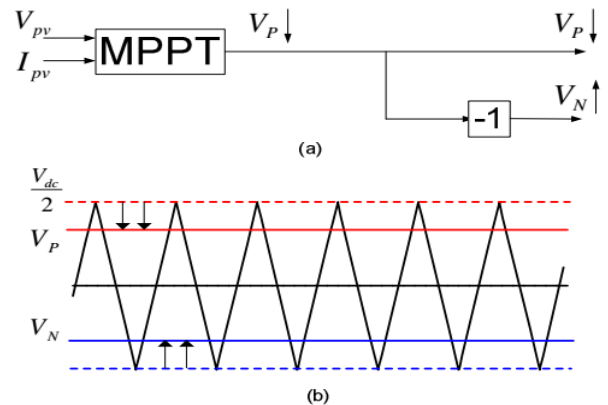
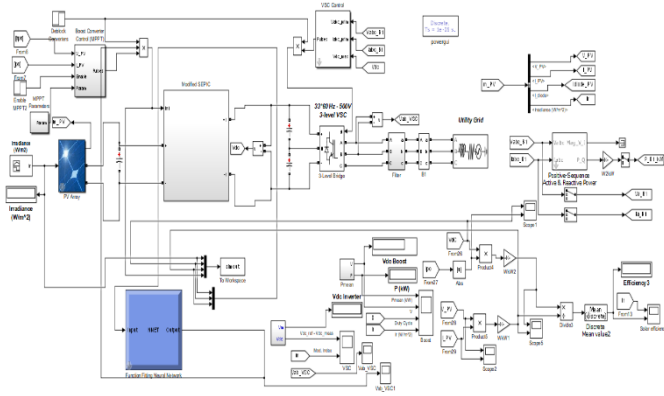


Fig. 15. MPPT scheme (a) block diagram and (b) simple boost scheme

#### V. SIMULATION OF THE QZSI WITH PV INTERFACE

The simulation model of the proposed PV based qZSI is illustrated in Fig. 16. To calculate the results of the qZSI it is intended in MATLAB/SIMULINK and the experimental waveforms are obtained. The performance of the inverter is studied under steady-state conditions. The performances of the systems are validated with the models to their efficiency conditions.

# Quasi Z-Source Inverter for Pv Power Generation Systems



**Fig. 16. Simulation diagram of the proposed qZSI**

This simulation contains MPP tracking and battery charger circuit. This design converts the input dc from the PV module into a 3-phase AC voltage. It boosts up the amplitude even the input PV voltage is minimum. The output of the proposed inverter can be given to the main grid through the grid interfacing circuit. The design of the grid interfacing unit and the MPPT control is presented in Fig.17.

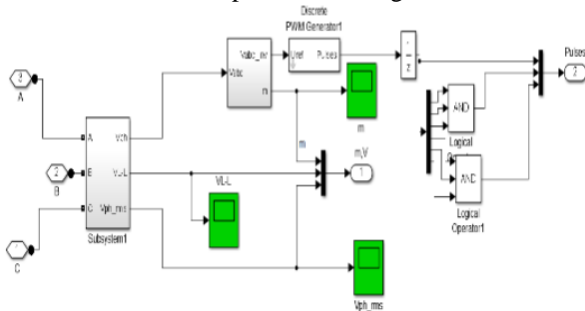


**Fig.17. Grid interface and MPP control of the proposed qZSI inverter**

The bidirectional control system employed for battery storage in the proposed configuration is designed and the respective simulation diagram is depicted in Fig. 18. The voltage is boosted using the boost converter with the help of a PWM switching.

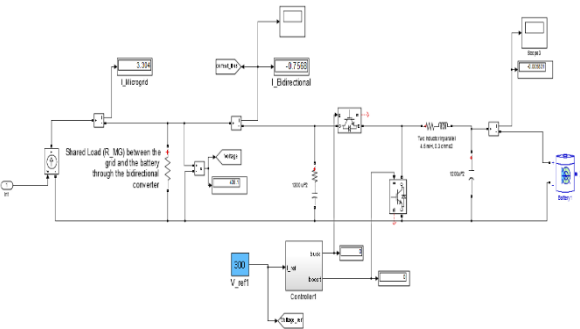


**Fig. 18 Simulation of bidirectional controller**

## VI. RESULTS AND DISCUSSIONS

The applied voltage and the respective output voltage obtained from the simulation are illustrated in Fig. 19-22. Moreover, the values are tabulated in Table III. This implies that the voltage is boosted is controlled by using the control circuit according to the voltage obtained from the PV module (which is given as input to the proposed qZSI converter).

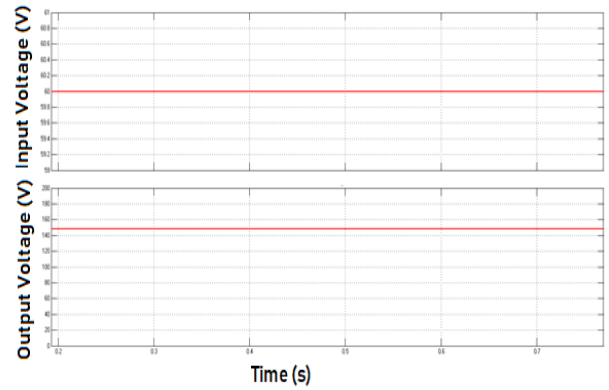


**Fig. 19. qZSI output voltage when the input voltage is 60V**

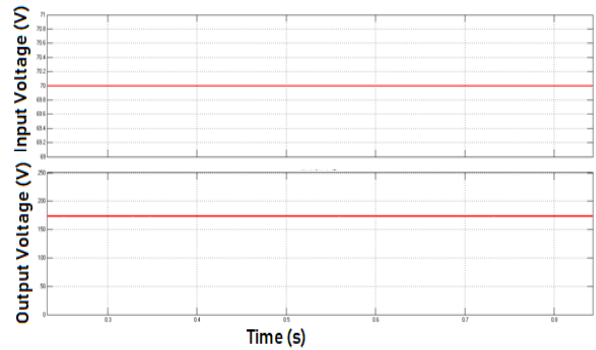


**Fig. 20. qZSI output voltage is boosted when the input voltage is 70V**

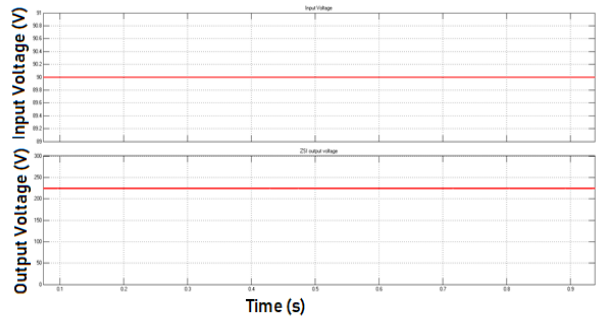


**Fig. 21. qZSI output Voltage when the input voltage is 90V**

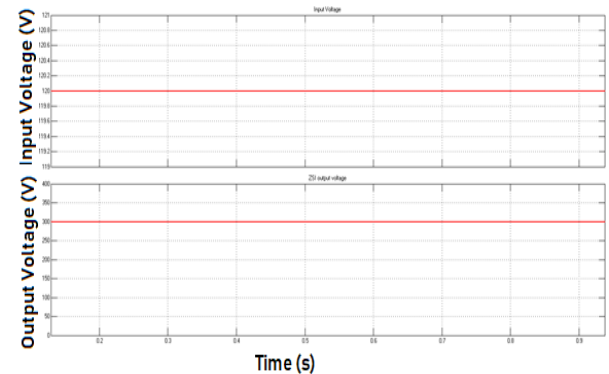


**Fig. 22. qZSI output voltage vs. input voltage is 120V**

The input voltages and the corresponding voltages of qZSI are shown in Table III.

**Table III Input voltage and the corresponding boost voltage**

Input Voltage (V)	Boost Voltage (V)
60	148
70	173
90	223
120	300

As depicted in Table III, though the input varies, the output is boosted to 500V by adjusting the gain value using the control circuit.

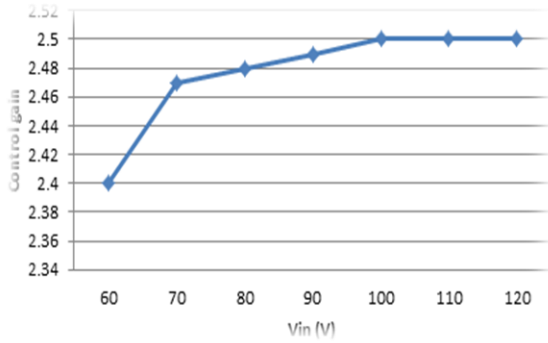


**Fig. 23. Input voltage and gain**

This is illustrated using Fig. 23, which shows the gain values for the different input voltages. In Fig. 24 is depicts the capacitor voltage 1, 2 and current in inductor.

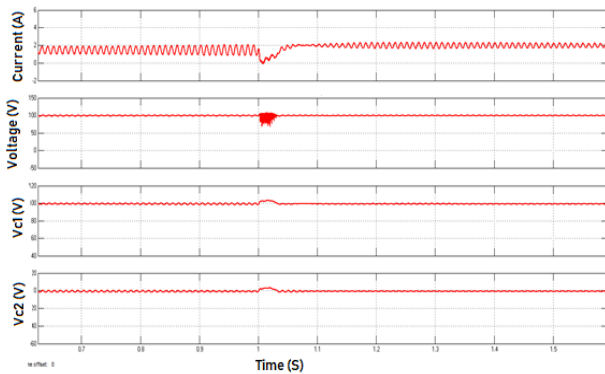


**Fig. 24. Inductor current and voltages across the capacitors C1 and C2 of the Z source network**

The three phase output voltage and the three phase current at the inverter are depicted in Fig. 25. The control circuit also regulates the dc-link voltage using the control circuit. The PI controller alters the gain to regulate the dc-link voltage. The output of the inverter is filtered by the LCL filter and after a current regulator is to adjust the current output of the inverter to maintain maximum power delivery. Dc-link regulation is depicted in Fig. 26.

The variation of the modulation index tends to change the  $V_{out}$ . The output of the qZSI is kept at 330V. From the above control, the voltage output is boosted to maintain constant ac voltage. From Fig. 26 it can be observed that the solar voltage even under the solar variation levels the voltage output of the converter is maintained around 230V and the qZSI tends to operate under constant voltage generation mode based on the variation of the solar irradiance. The difference of the solar irradiance happened at the 1s.

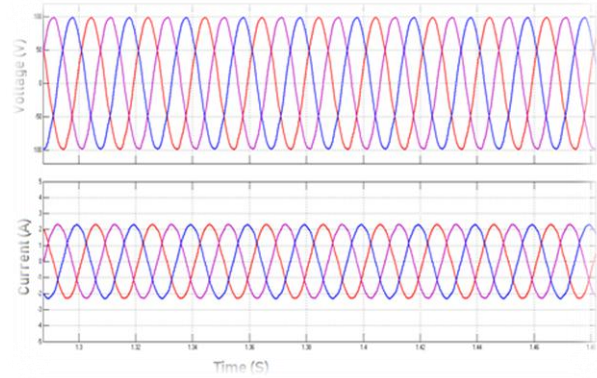


**Fig. 25. Three-phase voltage and current**

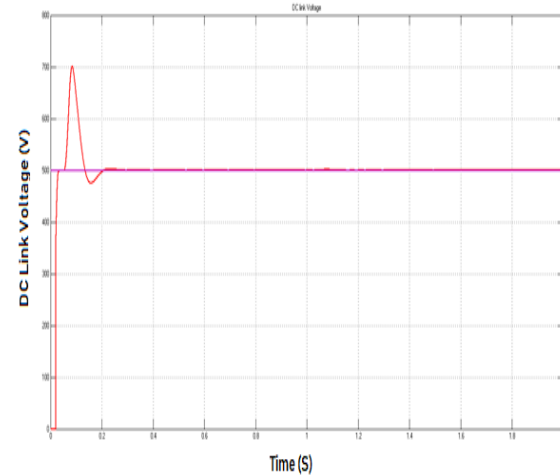


**Fig. 26. DC-Link voltage regulation**

Fig. 27 depicts the in-phase voltage and current. The input voltages and the respective battery voltages are depicted in Fig. 28 whereas the battery voltages and the SoC voltage are depicted in Fig. 29. The input voltages and the efficiency of the proposed configurations are shown in Fig. 30. The efficiency values are 86, 84, 82, 80, 80, 78, 76 when the voltages are 60V, 70V, 80V, 90V, 100V, 110V and 120V, respectively. The sinusoidal current at the grid side is maintained with the help of suitable filters.

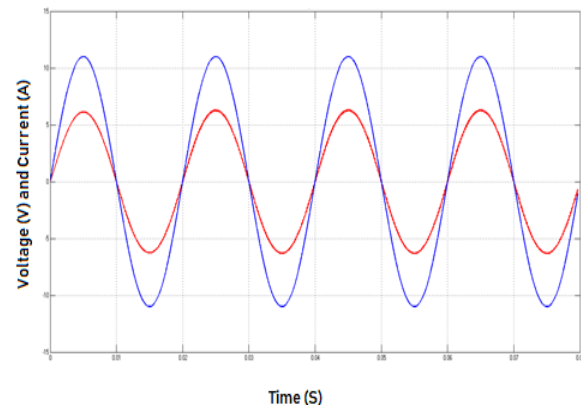


**Fig. 27. Inphase voltage and current**

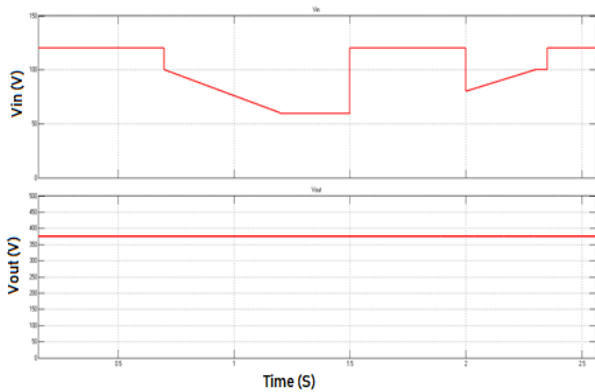


Fig. 28. Input and battery voltage

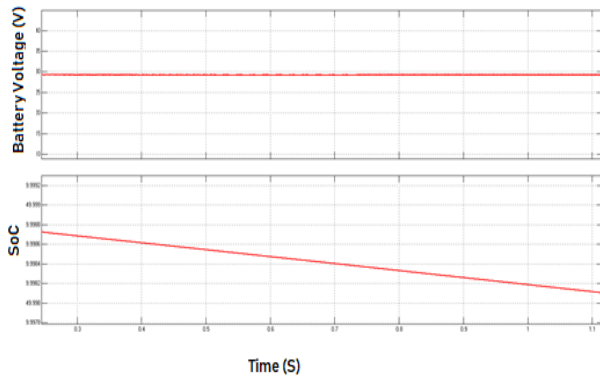


Fig. 29. Battery voltage and SOC

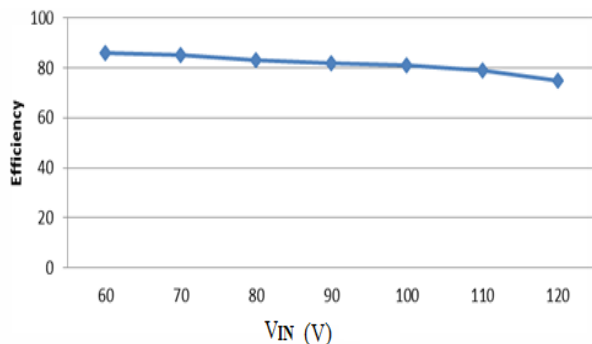


Fig. 30.  $V_{in}$  and efficiency

It can be observed that the solar voltage changes from 100V to 230V, the inverter is still operated with 230V constant and as the input varies the MPP tracker with the voltage mode control regulates the output voltage to constant in order to maintain line voltage as fixed. The input dc source is fed to the qZSI, is operated under the non-shoot through state control; the input voltage of the PV panel is slatted and stored in the capacitors evenly around 100V and it is combined to obtain a voltage around 200V which is fed to the battery in parallel. The inductor current seems to be sinusoidal which oscillates for the peak current around 2A. It is being disturbed by the source power change that has occurred in 1 sec, where the load voltage is kept around 100V. The MPP tracker reacts fast to maintain the steady-state and regulates the PCC current to stabilize the line voltage.

## VII. CONCLUSION

To validate the performance of the inverter, the model of

qZSI has been designed and simulated in MATLAB/SIMULINK package. Also a bidirectional battery storage scheme is designed and added in the system block. The work discusses mainly on the method of storage battery connection and the power flow management at different modes of operations. This design converts the input dc from the PV module into 3-phase AC voltage. It boosts up the voltage even the input PV panel voltage is low. The output of the proposed inverter can be given to the main grid through the grid interfacing circuit. The output is varied by adjusting the gain value using the control circuit. The output voltage is boosted by the qZSI and excess power was stored in the bidirectional battery charger. Also the efficiency of the system is checked by output voltage corresponds to its input voltage. The system gives the high boost conversion ratio, also MPPT method gives the maximum power from PV. The input fed to the qZSI is kept around 200V, as the qZSI operates in non-shoot through the state that brings the voltage output equal to the input voltage, and it is around 200V. The variation of the modulation index tends to change the output voltage of qZSI and is boosted to 330V.

## REFERENCES

1. Sathishkumar, R, Malathi, V & Deepamangai, P 2016, 'Quazi Z-source inverter incorporated with hybrid renewable energy sources for microgrid applications', in Journal of Electrical Engineering, vol. 16, pp. 458-467.
2. Akagi, H, Kanazawa, Y & Nabae A, 1983, 'Generalized theory of the instantaneous reactive power in three-phase circuits,' in Proc. Int. Power Electron. Conf. (JIEE IPEC), Tokyo, Japan, pp. 1375-1386.
3. Anderson, J & Peng, FZ 2008, 'Four quasi-Z source inverters', Proceedings of IEEE PESC, pp. 2743-2749.
4. Andrade Antonio, MSS, Beltrame Rafael, C, Schuch Luciano & Martins Mario, LS 2014, 'PV module-integrated single-switch DC/DC converter for PV energy harvest with battery charge capability', IEEE Transactions on Power Electronics, vol. 66, pp. 439-447.
5. Antonio Augusto Frohlich, Eduardo Augusto Bezerra & Leonardo Kessler Slongo 2014, 'Experimental analysis of solar energy harvesting circuits efficiency for low power applications', Journal of Computers and Electrical Engineering Elsevier, vol. 45, pp. 143-152.
6. Antonio Augusto Frohlich, Eduardo Augusto Bezerra & Leonardo Kessler Slongo 2014, 'Experimental analysis of solar energy harvesting circuits efficiency for low power applications', Journal of Computers and Electrical Engineering ELSEVIER, vol. 45, pp. 143-152.
7. Mojtaba Forouzesh, Yam, P, Siwakoti, Saman, A & Gorji 2017, 'Step-up DC-DC converters: A comprehensive review of voltage-boosting techniques, topologies, and applications', IEEE Transactions On Power Electronics, vol. 32, pp. 12-18.
8. Sathishkumar, R, Chandrasekar, V & Malathi, V 2018, 'Analysis of solid-state transformer interfaced with renewable energy systems in microgrid', in the Journal of Electrical Engineering, vol. 18, pp. 20-30.
9. Yoshimoto, K, Nanahara, T & Koshimizu, G 2006, 'New control method for regulating state-of-charge of a battery in hybrid wind power/battery energy storage system', IEEE PES, vol. 37, pp. 1244-1251.
10. Ge, B, Abu-Rub, H, Peng, FZ, Lei, Q, De Almeida, AT, Ferreira, FJTE, Sun, D & Liu, Y 2013, 'An energy-stored quasi-Z source inverter for application to photovoltaic power system', IEEE Transactions on Industrial Electronics, vol. 60, no. 10, pp. 4468-4481.

## AUTHORS PROFILE



**Dr. R. Sathishkumar**, currently working as an Associate Professor in Pragati Engineering College, Andhra Pradesh, India in the department of Electrical and Electronics Engineering. He completed his Ph.D. in Anna University, Chennai, a master's degree in power systems engineering in Government College of Technology,

Coimbatore and undergraduate in Sethu Institute of Technology, Madurai. His current research interests are renewable energy systems, power systems, and microgrid. Email id: rskgct@gmail.com.



**Dr.R.Velmurugan** completed his Bachelor of Engineering (EEE) in 2001 at PSNA College of Engineering and Technology, Dindigul (Madurai Kamaraj University, Madurai). He received the Master of Engineering (PE &D) at PSNA College of Engineering and Technology, Dindigul (ANNA University, Chennai) in 2006. He completed his Doctorate in Philosophy, Anna University, Chennai, India in 2018. He is currently working as a Professor of EEE department at Malla Reddy Engineering College for Women, Secunderabad, Hyderabad. His areas of interest are Power Electronics, Special Electrical Machines, Electric Drives & Control, and Power Quality. He is a Life Member of Indian Society for Technical Education. Email id: velsvictor@gmail.com.



**Dr.Balakrishnan Pappan** obtained his Bachelor's degree in Electrical and Electronics Engineering from Government College of Engineering, Affiliated to Periyar University, Salem and Master's degree in Embedded Systems Technologies from K.S.R. College of Engineering, Tiruchengode, Affiliated to Anna University Coimbatore. He received his Doctorate of Philosophy under Faculty of Electrical Engineering, Anna University, Chennai, Tamilnadu in 2017. Currently, he is an Associate Professor, Faculty of Electrical and Electronics Engineering, Malla Reddy Engineering College for Women, Secunderabad, Telangana State. His areas of interest are soft computing techniques for power systems faults and embedded systems. His current research interests are power system optimization, renewable energy. Email id: bala4k@yahoo.com.



**Dr.J.Booma**, received B.E., Degree from Madurai Kamaraj University, Madurai, M.E., and Ph.D. from Anna University, Chennai, India. She is presently working as an Assistant Professor in the Department of Electronics and Communication Engineering, PSNA College of Engineering and Technology, Dindigul, India. She has presented papers in more than 30 National and International level conferences. She is having more than 10 publications in indexed Journals. Her field of interest is Power system planning, Electronics Circuits, Robotics, and Control Systems. She is a Life Member of ISTE. Email id: boomakumar2005@gmail.com.